Geochemistry Geophysics Geosystems G3
AN ELECTRONIC JOURNAL OF THE EARTH SCIENCES
Published by AGU and the Geochemical Society

Technical Brief
Volume 8, Number 1
5 January 2007
Q01001, doi:10.1029/2006GC001412
ISSN: 1525-2027

Topography and self-gravitation interaction in elastic-gravitational modeling

M. Charco
Instituto de Astronomía y Geodesia (CSIC-UCM), Fac. C. Matemáticas, Universidad Complutense de Madrid, Plaza de Ciencias, 3, Ciudad Universitaria, E-28040 Madrid, Spain (maria_charco@mat.ucm.es)

F. Luzón
Departamento de Física Aplicada, Universidad de Almería, Cañada de San Urbano s/n, E-04120 Almería, Spain (fluzon@ual.es)

J. Fernández
Instituto de Astronomía y Geodesia (CSIC-UCM), Fac. C. Matemáticas, Universidad Complutense de Madrid, Plaza de Ciencias, 3, Ciudad Universitaria, E-28040 Madrid, Spain (jose_fernandez@mat.ucm.es)

K. F. Tiampo
Department of Earth Sciences, University of Western Ontario, London, Ontario, Canada N6A5B7 (ktiampo@uwo.ca)

[1] Changes in gravity due to volcanic loading of the crust are influenced by topography. We investigate the relative importance of topography and self-gravitation in the interpretation of gravity changes. It is shown that modeling of gravity changes can be more precise with the introduction of topographic relief, although it is neglected self-gravitation of the medium. This paper exploits this result by suggesting a mathematical simplification that could be useful in the future development of a numerical technique to accurately include topographic effects in the modeling of deformation and gravity changes. Finally, we perform an inversion of the gravity changes observed at Mayon volcano (Philippines) between December 1992 and December 1996 including topographic effects by varying the depth of the source. Failure to account for topographic influences can bias estimates of source parameters particularly when the lateral extension of the relief is of the same order of magnitude as the source depth.

Components: 5107 words, 5 figures, 1 table.

Keywords: modeling; elasticity; self-gravitation; topography.

Index Terms: 0545 Computational Geophysics: Modeling (4255); 1217 Geodesy and Gravity: Time variable gravity (7223, 7230); 8419 Volcanology: Volcano monitoring (7280).

Received 6 July 2006; **Accepted** 11 September 2006; **Published** 5 January 2007.

Charco, M., F. Luzón, J. Fernández, and K. F. Tiampo (2007), Topography and self-gravitation interaction in elastic-gravitational modeling, *Geochem. Geophys. Geosyst.*, *8*, Q01001, doi:10.1029/2006GC001412.

1. Introduction

[2] Elastic half-space models have been widely used to interpret deformation and gravity changes in active volcanic areas. The most commonly used is the *Mogi* [1958] point dilatation model, although more refined models have also been introduced. These include finite shape spherical and ellipsoidal sources, vertical and horizontal magma migration, collapse structures, etc. [e.g., *Davis*, 1986; *McTigue*, 1987; *Bonafede*, 1990; *De Natale and Pingue*, 1996]. *Rundle* [1980, 1982] solves the generalized static Navier equations of an elastic self-gravitating layered half-space to obtain surface gravity, deformation and potential changes arising from volcanic loading. This type of model takes into account the intruding masses and their interaction with self-gravitation. *Charco et al.* [2006] carried out a dimensional analysis and theoretical experiments indicating that mass change and self-gravitation could produce changes in the value and pattern of predicted gravity that may be above microgravity survey accuracy. It is frequently possible to achieve microgravity measurements at high precision at volcanoes (±10–15 μGal) when following strict survey procedures [*Rymer and Brown*, 1989; *Williams-Jones et al.*, 2003]. All these models generally assume that variations in topography do not significantly affect deformation and gravity changes. However, volcanoes are often associated with prominent relief that can critically affect the deformation field [e.g., *Williams and Wadge*, 1998, 2000; *Cayol and Cornet*, 1998; *Folch et al.*, 2000]. Thus what should a model include to provide better insight into the interpretation of gravity changes? Elastic-gravitational models can provide a far more appropriate approximation than purely elastic models to problems of volcanic loading in which topographic relief can be negligible. However, for prominent volcanoes the general and local aspects of the ground surface also can affect deformation [e.g., *Williams and Wadge*, 1998, 2000; *Cayol and Cornet*, 1998; *Folch et al.*, 2000] and gravity changes.

[3] We use dimensional and scaling analysis to show theoretically the relative importance of topography and self-gravitation effects on displacement and gravity changes caused by volcanic loading (internal loading produced by pressure and mass changes). These dimensional arguments indicate a simple qualitative rule by which one can begin to assess the importance of topography on modeled displacements and gravity changes.

2. Deformation Model

[4] We begin by reviewing the coupled elastic gravitational model. The generalized static Navier equations for an elastic, self-gravitating and uniform medium are as follows [*Love*, 1911]:

$$\rho_o g \nabla(\mathbf{u}\cdot\mathbf{e}_z) - \rho_o \nabla\phi - \rho_o g \mathbf{e}_z \nabla\cdot\mathbf{u} + \nabla\cdot\sigma + \rho_o \mathbf{F}_p = 0 \quad (1)$$

$$\nabla^2\phi = -4\pi\rho_o G \nabla\cdot\mathbf{u} + \nabla\cdot\mathbf{F_m} \quad (2)$$

[5] Here, $\mathbf{u}$ is the vector displacement in a local cylindrical coordinate system (r, θ, z) with the origin at the surface and with the z axis pointing down into the medium, $\mathbf{e_z}$ is the unit vector in the z direction, ϕ is the gravitational potential, ρ_0 the unperturbed density, G is the gravitational constant and g is the acceleration of gravity. The state of equilibrium is slightly disturbed by the emplacement of a mass source, or a pressure source, or the combination of both, at some depth within the crust that will set up an additional stress field, σ. We have approximated the magma intrusion by the superposition of a spherical point source of dilatation, $\mathbf{F_p}$, and a mass point source, $\mathbf{F_m}$.

[6] *Rundle* [1980, 1982] solved equations (1) and (2) using the propagator matrix technique [*Thompson*, 1950; *Haskell*, 1953] in a flat layered, self-gravitating half-space to obtain surface gravity, deformation and potential changes arising from volcanic loading. *Rundle* [1981] developed the numerical formulation for the case of a single layer in welded contact with an infinite half-space. Expressions in the case of two layers are given by *Fernández and Rundle* [1994a, 1994b]. *Fernández et al.* [1997] gave the appropriate formulation for a medium composed of up to four layers over a half-space. More recently, *Charco et al.* [2002] obtained the analytical expressions to compute vertical deflection and geoid changes in a flat layered, self-gravitating half-space.

3. Scaling Relations

[7] We define the elastically perturbed gravitational potential after the intrusion of mass into the magma reservoir:

$$\phi = \phi_1 + \phi_2 \quad (3)$$

where ϕ_1 is the potential due to mass redistribution from the perturbed density, $\rho_o\nabla \cdot \mathbf{u}$, hereafter perturbed density potential, and ϕ_2 is the gravitational potential due to the influx of magma into a subvolcanic storage system, i.e., $\mathbf{F_m} = \nabla\phi_2$ (hereafter intruded mass potential). Elastic-gravitational model equations (1) and (2) are coupled through the perturbed density potential.

[8] *Charco et al.* [2006] point out that changes in the magma pressure drive the deformation. Since it makes little difference whether the mass source is used to calculate displacements, gravitational effects can be neglected to compute surface displacements at spatial scale associated with volcano monitoring. However, with two sources of loading, mass and pressure, it is possible to reproduce the unusual geodetic data observed at certain volcanoes; total uplift may vanish without total gravity change vanishing, combining mass and pressure in a suitable way [*Rundle*, 1982]. Considering both types of sources, *Charco et al.* [2006] point out that the potential ϕ_1 is of the same order of magnitude as the intruded mass potential, ϕ_2, at spatial scale associated with volcano monitoring. Therefore the gravitational terms that appear in equation (1) may contribute to the magnitude of gravity changes since both equations, (1) and (2), are coupled. In fact, gravitational effects can produce significant variations in the magnitude and pattern of the gravity change for half-space models. Following this study, here we investigate the relative importance of topography and self-gravitation in gravity changes modeling.

[9] It can be anticipated that the interaction of the perturbed density potential with topography is strongest for sources located at shallow depths. Considering equations (1) and (2), the perturbed density potential scales like

$$\nabla\phi_1 \sim \frac{|\mathbf{u}|}{c} \tag{4}$$

since it depends on $\nabla \cdot \mathbf{u}$. For this dimensional analysis, it is assumed that the depth of the source, c, characterizes the distance scale over which the solution varies. The intruded mass potential, ϕ_2, scales like $\Delta V/c^3$, where ΔV is the change in volume that produces the magma chamber overfilling. *Delaney and McTigue* [1994] pointed out that

$$\Delta V \simeq 4\pi a^2 \Delta a \tag{5}$$

where Δa is the change in cavity radius. Therefore

$$\nabla\phi_2 \sim \frac{a^2\Delta a}{c^3} \tag{6}$$

[10] The magnitude of both potentials decreases with increasing depth. As the magnitude of potential ϕ_1 depends on expression (4) and the magnitude of potential ϕ_2 depends on (6), the intruded mass effect decreases faster with depth than perturbed density potential effect.

[11] We use expressions (4)–(6) to describe the topographic effect on gravity changes. We assume that the topographic effect is due primarily to differences in the distance between surface and source location, i.e., it is due to the height of the computation point since gravity is strongly height dependent [e.g., *Torge*, 1989]. Therefore the higher the topography, the deeper the source. This assumption gives a reasonable approximation since the principal effect of ground topography is a reduction of displacement in regions of elevated topography [*Williams and Wadge*, 1998, 2000]. This is due to the greater distance from the free-surface and the fact that gravity changes are primarily controlled by (1) the change in vertical displacement due to inflaton/contraction, (2) the change in vertical displacement due to the deformation induced by a point mass load within the medium, and (3) the change in mass produced by introduction of the point load, where gravitational attraction primarily depends on distance between the computation point and the intruded mass source rather than the local shape of the free surface. Elastic and gravitational forces in the elastic gravitational model depend on source depth [*Battaglia and Segall*, 2004; *Charco et al.*, 2006] and therefore also depend on the distance between the surface and source location.

[12] Topography is included in the scaling relations by replacing source depth by c', where $c' = c + f(r, \theta)$. The term f, which is a function of radial distance, r, and azimuth angle, θ, in the local cylindrical coordinate system, is the elevation above mean sea level. Taking into account the relief, the ratio between the first and second term of the right-hand side of equation (2) is

$$\frac{\nabla\phi_1}{\nabla\phi_2} \sim \frac{|\mathbf{u}||c'|^2}{a^2\Delta a} \tag{7}$$

[13] Topography has a significant effect on the magnitude of the predicted gravity changes since

ratios (4) and (6) and consequently (7), are functions of the relief elevation. For a deep source, $c \geq 10$ km ($c/c' \simeq 1$) the topographic effect is small. However, the magnitude of changes in gravity arising from both potential ϕ_1 and potential ϕ_2 are not significant within typical standard deviations on microgravity measurements in this case. Thus, although topographic influence on gravity is not significant for either ϕ_1 or ϕ_2, the magnitude of both potentials is too small to be considered. For a shallow source, $c < 10$ km ($c/c' \ll 1$) both potentials are affected by topography since c and the height of the topographic relief are of the same order of magnitude in this case, e.g., considering mean heights above mean sea level of 3 km. The reduction of the magnitude of relations (4) and (6) can be significant due to topographic effects since $c \ll c'$. The magnitude decrease that both potentials undergo produces a drop in the gravitational forces acting on equations (1) and (2) because the distance of the source to the free surface increases with topography. Thus the error caused by neglecting gravitational terms in equation (1), that may contribute to the magnitude of gravity change in half-space models, can be neglected when topography is taking into account. Consequently, topography reduces the magnitude of self-gravitation effects due to the superposition of a pressurized cavity and intruded mass, particularly for magma reservoirs at relatively shallow depths.

[14] *Folch et al.* [2000] pointed out that topography effect on the displacement field is dramatically emphasized in viscoelastic rheologies. Self-gravitation and gravitational acceleration could significantly affect both displacements and gravity changes in such a case. Thus it remains to be seen whether this approach may be extended to viscoelastic modeling.

4. Self-Gravitation and Topography Interaction

[15] We perform theoretical experiments that examine the relative importance of self-gravitation and topographic effects by using the elastic-gravitational model. We show the results for sources at 5 (Figure 1), 15 (Figure 2), and 30 (Figure 3) km depth in a homogeneous medium with Lamé parameters $\lambda = \mu = 30$ GPa and density $\rho = 3000$ kg m^{-3}. Following the assumptions made to perform the dimensional analysis, the experiments are carried out considering (1) the effects on gravity changes due to a pressurized magma chamber of 300 MPa km^3 strength with no mass change, (2) the effects due to a spherical mass point of 0.35 MU (1 MU = 10^{12} kg) with no magma chamber overpressure, and (3) the superposition of the effects due to sources described in considerations 1 and 2. In this case, both sources have the same influence on equation (2), producing changes in gravity at the same magnitude and a different sign. Furthermore, to study the effect of topographic relief, we consider four different approximations: (1) a half-space without topographic relief (Model 0); (2) a horizontal free surface with a constant elevation of 3 km corresponding to a "representative elevation" [see, e.g., *Bonaccorso*, 1996] for a volcanic area (Model 1); (3) an axisymmetrical volcano with average slopes of the flanks of 60° that could be representative of andesitic volcanoes (Model 2); and (4) an axisymmetrical volcano with average slopes of its flanks of 25° that could be representative of basaltic shield volcanoes (Model 3). The maximum height of the axisymmetrical volcanoes is 3 km, providing lateral extensions of topography (horizontal distance from summit to the flank of topographic relief) of 0.5 and 6 km, respectively. Gravity changes created by sources located beneath axisymmetrical volcanoes, cases 3 and 4, are obtained by allowing the source depth to vary with the elevation of the point at which a solution is desired, as introduced by *Williams and Wadge* [1998], to be consistent with the assumptions we made to perform the dimensional analysis.

[16] The solution corresponding to the volcanoes with an average slope of 25° (Model 3) and 60° (Model 2) are midway between that of a half-space solution (Model 0) and that of a constant elevation of the free surface (Model 1). Surface gravity changes vary rapidly in a narrow region with a half-width similar in magnitude to source depth, c [*Rundle*, 1981]. There are not significant variations of the region when the topographic lateral extent is less than region width, as it can be seen for Model 2 in Figure 1 and for Models 2 and 3 in Figures 2 and 3, respectively. Therefore the interaction of the source-induced gravity changes with topographic relief is significant only when source depth and the lateral extension of the relief are of the same order. *McTigue and Segall* [1988] reached a similar conclusion which respect to the conditions under which a subsurface deformation source and topography interact most strongly.

[17] The topographic effect on the magnitude of predicted gravity changes is higher for sources located at relatively shallow depths. Thus, for a

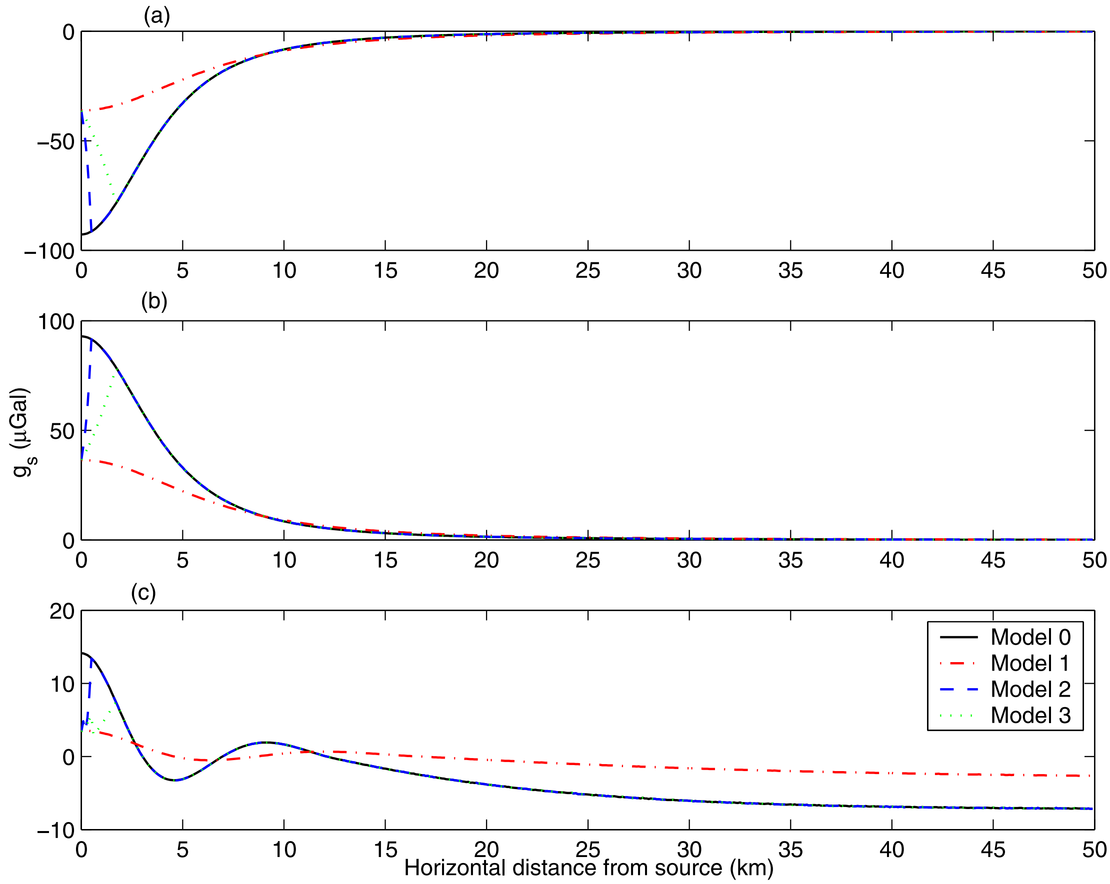

Figure 1. Source located at c = 5 km within a homogeneous medium with $\lambda = \mu = 30$ GPa. (a) Surface gravity change (μGal) due to a center of dilatation of 300 MPa km^3. (b) Surface gravity change (μGal) for a spherical mass source of 0.35 MU. (c) Surface gravity caused by the superposition of both sources. Topographic features are different for each volcanic area, but as an approximation we assume that Model 0 represents a homogeneous half-space; Model 1 represents a representative elevation of 3 km reference height; Model 2 represents an axisymmetrical volcano with average slopes of their flanks of 25°; and Model 3 represents an axisymmetrical volcano with average slopes of their flanks of 60°. (See text for more details.)

model with a dilatational source at 5 km depth (Figure 1a), the surface gravity change is reduced by as much as 61% if topography is taken into account and as much as 30% for a model with a dilatational source at 15 km depth (Figure 2a). This reduction of magnitude is approximately of 15% if the dilatational source is at 30 km depth (Figure 3a). A similar reduction can be seen for the point source of mass (Figures 1b, 2b, and 3b). In summary, for shallow source (5 km) compared to the topography, there is a significant and measurable topographic effect on gravity changes. For the deeper source the effect is unmeasurable, i.e., the reduction of the magnitude of gravity changes tends to 0 as the source depth increases ($c/c' \simeq 1$). This fact is consistent with the theoretical results pointed out above.

[18] The elastic-gravitational model includes self-gravitation of the Earth through coupling between equations (1) and (2). We have computed the superposition effect of both sources described above in order to consider the topographic effect on surface gravity changes due to self-gravitation (Figure 1c, Figure 2c, and Figure 3c). Mass interaction with the gravity field is noticed at horizontal distances on the order of the source depth. Dimensional arguments indicate that the reduction of self-gravitation with topographic relief is strongest for sources that are shallow compared to the topography. The coupling effect is reduced by approximately 71% for the model with the gravitational source located at 5 km beneath a volcanic cone with 25° flank slope (Figure 1c, Model 3) and by 50% if the source is located at 15 km depth

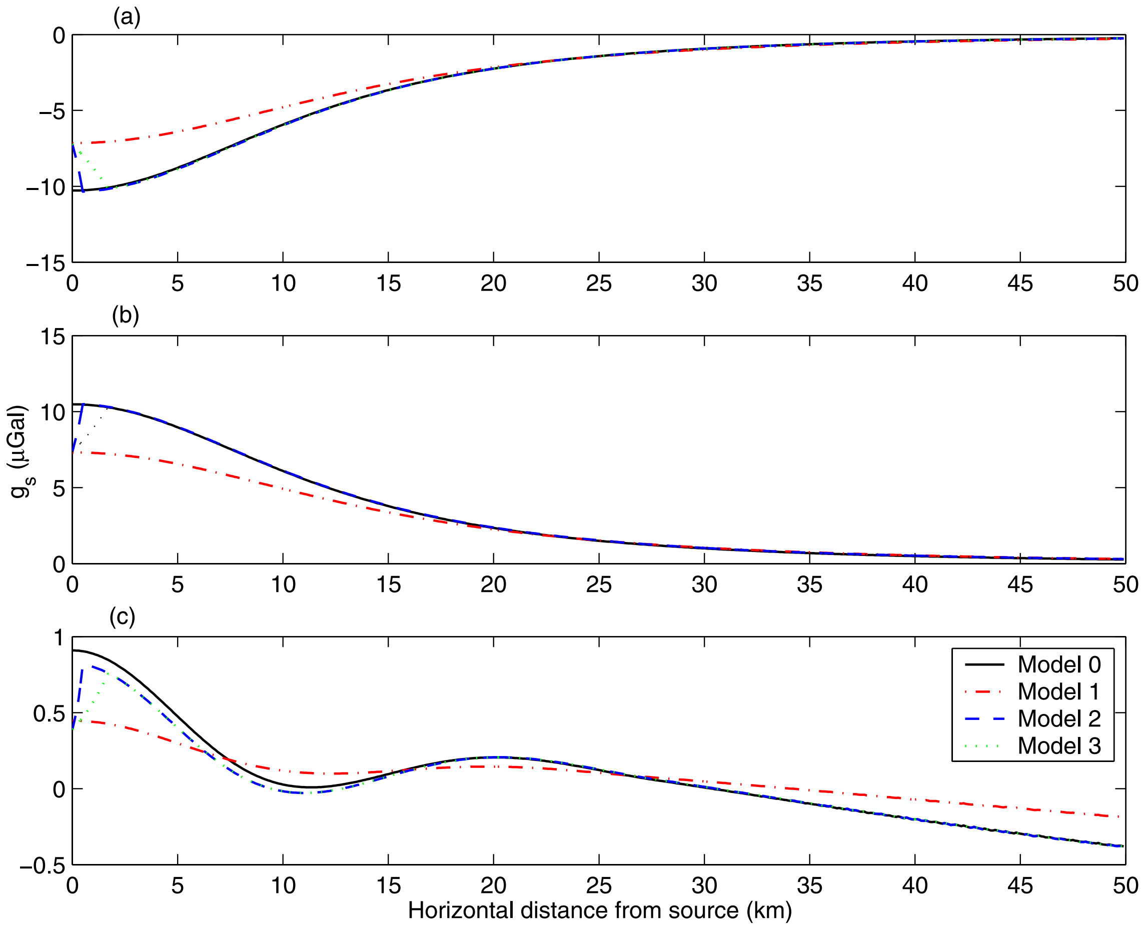

Figure 2. The same as Figure 1, but the source is located at 15 km depth.

(Figure 2c, Model 3). Thus topographic effects on self-gravitation decrease with increasing source depth. Nevertheless, the fractional change decreases slowly with increasing depth since potential ϕ_1 depends on $1/c'$ while ϕ_2 depends on $1/c'^3$. For magma reservoirs at relatively shallow depths ($c/c' \ll 1$), that could produce coupled signals within the accuracy attainable nowadays in microgravity surveys, topography has a significant effect masking self-gravitation effects. For deep sources, the coupled signal is too small to be discernible from the background noise. Therefore noncoupled solutions that take into account topographic relief are more accurate than a coupled solution in a half-space for typical source depths in volcanic areas. In this way, we can reduce (1) to the vector static Navier equation:

$$\nabla \cdot \sigma - \rho_o \nabla \phi_2 + \mathbf{F}_p = \nabla^2 \mathbf{u} + \frac{1}{1 - 2\nu} \nabla \nabla \cdot \mathbf{u} - \rho_o \nabla \phi_2 + \mathbf{F}_p = 0 \tag{8}$$

where ν is Poisson's ratio. Topographic contributions to gravitational potential gradient are implemented in the change in vertical displacement induced by chamber inflation/contraction and by the point mass load within the medium. The topographic effect on the gravity changes caused by the change in mass can be represented by varying the source location with the point elevation.

5. Application

[19] We use the varying depth methodology to interpret geodetic observations made at Mayon, a classic stratovolcano cone with an altitude of 2462 m. Mayon is the most active volcano in the Philippines, located in the Bicol volcanic chain southeast of the island of Luzon, Philippines, part of the Legaspi Lineament of the central Philippine fault system, which runs NW-SE across Legaspi City [*Jentzsch et al.*, 2001]. Since 1616, this volcano has erupted 47 times and nearly every

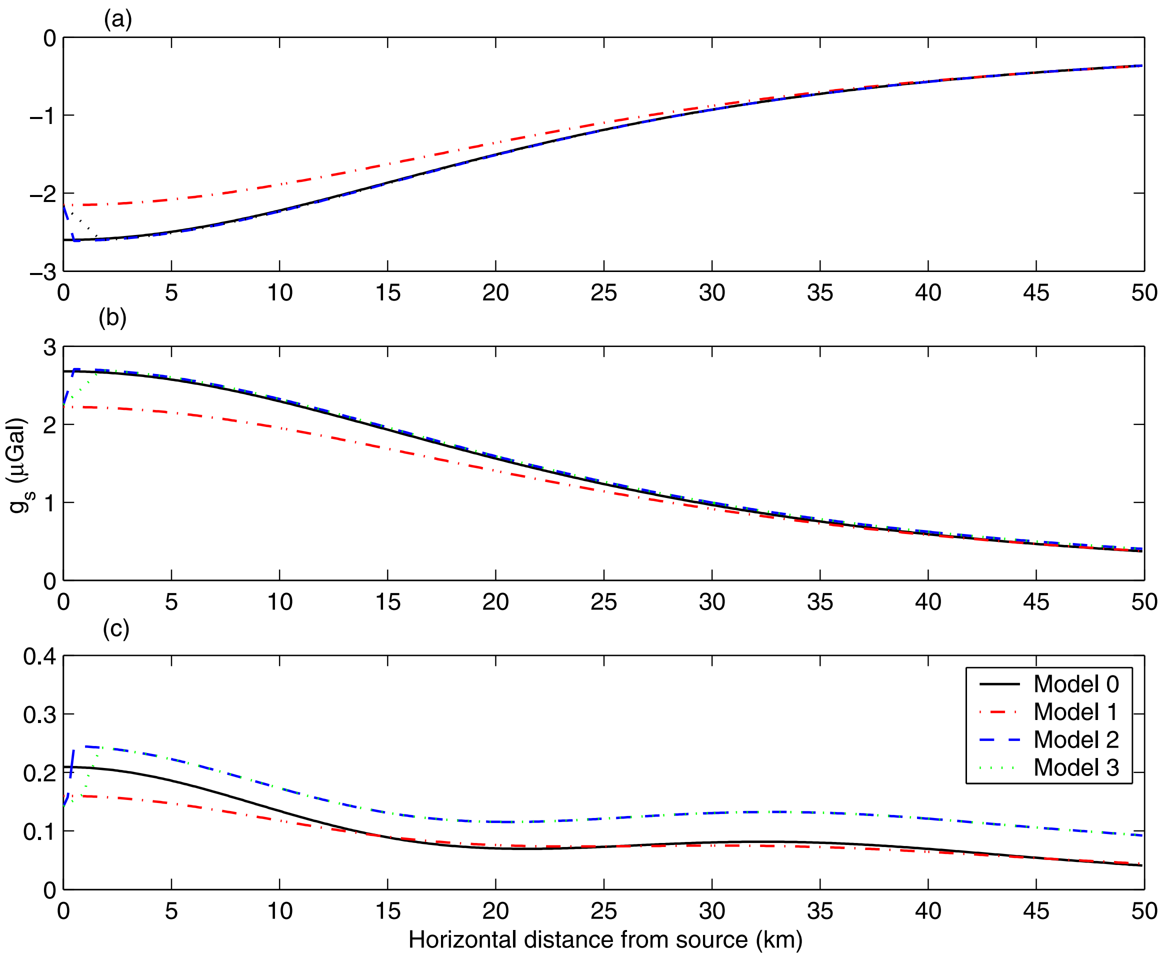

Figure 3. The same as Figure 1, but the source is located at 30 km depth.

10 years during the last century. The last strong eruption was in 1984, the youngest one in 2001 [*Jentzsch et al.*, 2004]. Due to the population density in the area, it has been monitored more closely in recent years [*Punongbayan et al.*, 1990; *Völksen and Seeber*, 1995; *Jahr et al.*, 1998; *Jentzsch et al.*, 2001].

[20] Five microgravity and differential GPS surveys were carried out between December 1992 and December 1996. The measurements were conducted along two profiles located on the flanks of the volcano toward the summit. These profiles are connected to a local and a regional network installed around the volcano. The reference network, which is formed by a total of 26 stations, is connected to two points at the opposite side of Legaspi Lineament [*Jentzsch et al.*, 2001].

[21] In early 1993, just after the start of gravity measurements in December 1992, an eruption occurred, with ash fall and lava flow of approximately 10 million m^3 [*Withman*, 2005]. Despite the activity in 1993, there was no significant gravity change between the first and second campaign (December 1992, May 1993). The gravity increase between May, 1993 and December, 1996 reached almost 150 μGal ($\pm$14 μGal), increasing with elevation and decreasing with distance from the crater. Note that detailed discussion of the effect of groundwater on gravity measurements is given by *Jentzsch et al.* [2001]. The resulting conclusion is that the estimated maximum effect due to water level changes are on the order of 50 μGal on the lower slopes of the volcano. There remains therefore a significant residual gravity signal to be explained near the volcanic crater.

[22] The microgravity measurements for Tumpa-Lahar-Channel profile are shown in Figure 4. The gravity changes between each campaign and the first one (epochs 2–1, 3–1, 4–1, and 5–1) are restricted to a radius of 8 km around the volcano summit. During the campaigns, differential GPS did not recognize significant elevation changes

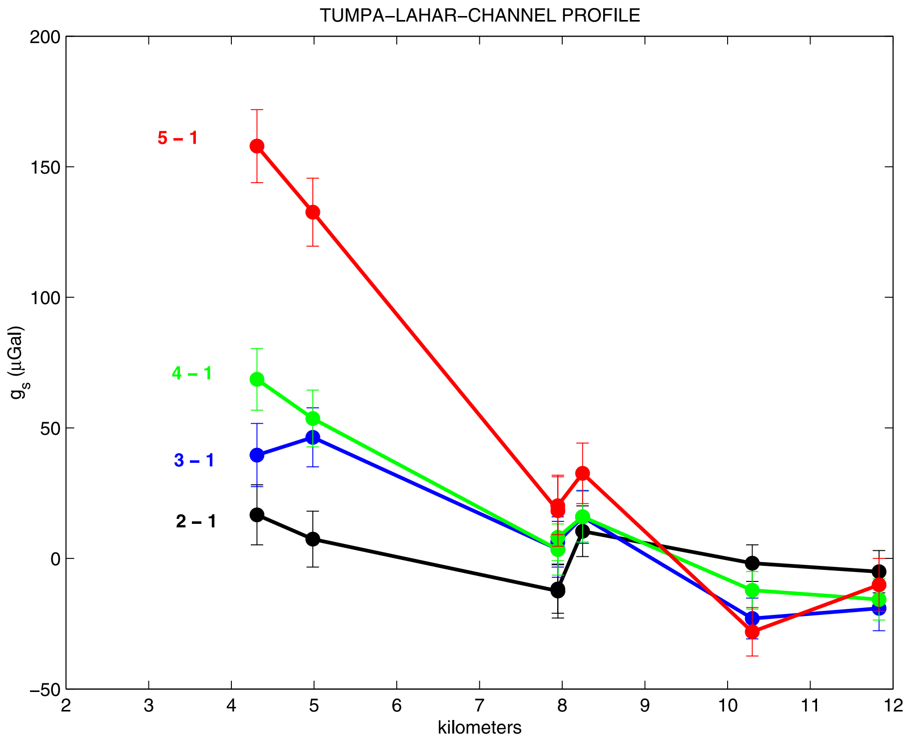

Figure 4. Gravity variations over the horizontal distance from the crater for the Tumpa-Lahar-Channel profile and epochs 2–1, 3–1, 4–1, and 5–1.

within their accuracy of ± 3 to 4 cm [*Jentzsch et al.*, 2001]. Volcanic activity dropped during this period, and remained dormant until the end of 1999. Gravity changes drawn against height differences from one campaign to the next show no gradient in Mayon, while it is unusual for gravity to increase with decreasing activity [*Jentzsch et al.*, 2001].

[23] *Jahr et al.* [1998] and *Jentzsch et al.* [2001] explained gravity changes observed at Mayon volcano as density changes within the vent system. The last eruption of Mayon volcano gave rise to the assumption that had been taken place a reinjection of mass into existing cavities instead of deflation. *Fernández et al.* [2001], *Tiampo et al.* [2004a], and *Tiampo et al.* [2004b] tested this hypothesis by modeling the changes in gravity without resolvable deformation using the Genetic Algorithm (GA) inversion technique [e.g., *Michalewicz*, 1992; *Tiampo et al.*, 2000] and the elastic-gravitational model that allows for the joint inversion of deformation and gravity data. The parameters obtained from the inversion through GA inversion are: a depth of 1.82 km, 31 MPa pressure increase, a radius of 1.71 km and 0.841 MU mass increase for changes in gravity observed during December 1992 and December 1996. Then, we have both pressurization together with mass injection. These parameters correspond to low-density value estimated; i.e., if we compute chamber volumetric expansion assuming that it is equal to the volume of magma that enters or leaves the cavity, it yields a low-density for the intruding mass.

[24] We perform a new inversion by using the varying depth methodology and an elastic model. Table 1 shows the predicted parameters and its comparison with the ones obtained by *Fernández et al.* [2001]. The best fitting model (Figure 5) suggests a shallow source with a positive mass increment. The radius estimated by using varying depth methodology to approach topographic effects increases density providing a more realistic value. However, we have to take in mind that this problem deals primarily with gravity effects due

Table 1. Source Parameters Obtained From the GA Inversion

	Elastic-Gravitational Half-Space	Varying Depth Methodology
Depth, *c*, km	1.82	2.17
Increment magma pressure, MPa	31	18.1
Radius, km	1.71	0.016
Mass increment, MU	0.841	0.6

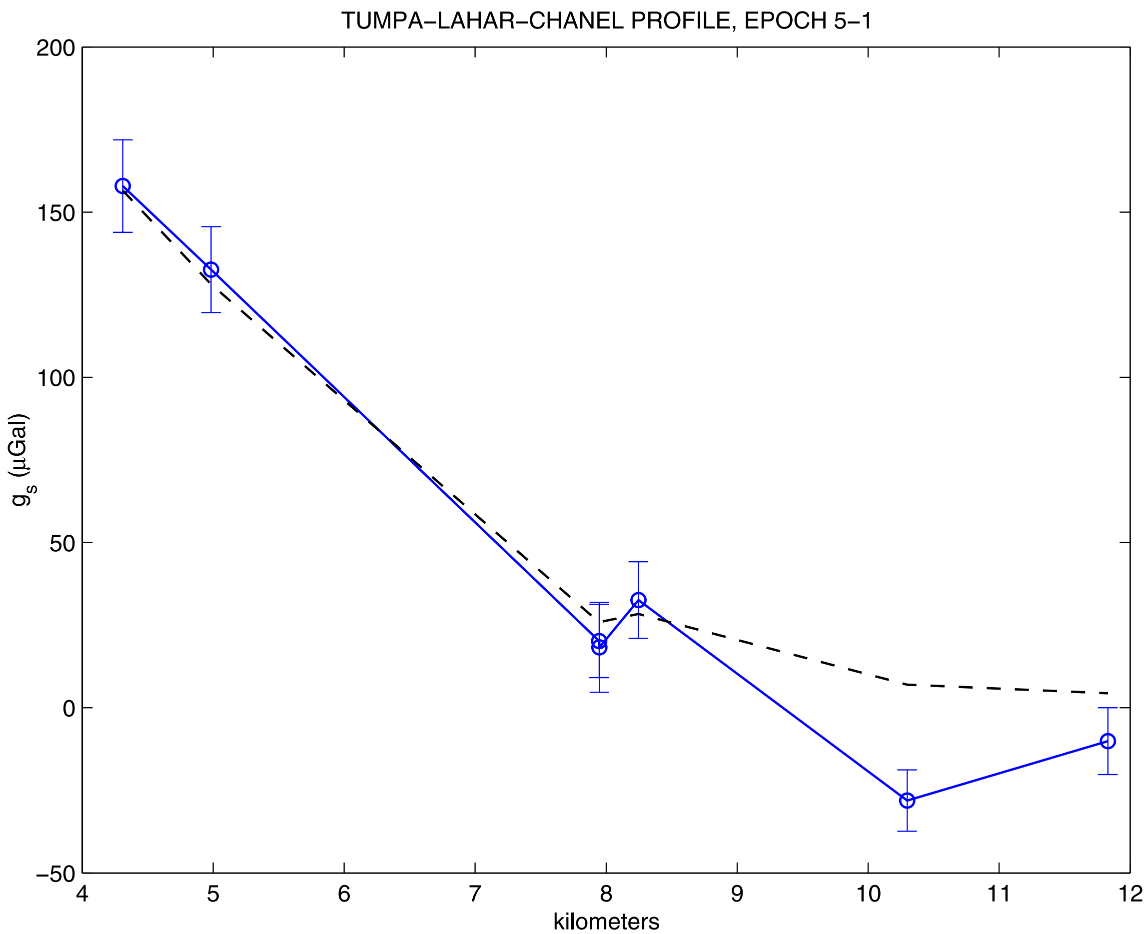

Figure 5. Measured values in the epoch 5–1 for the Tumpa-Lahar-Channel profile (solid line), and inversion results using varying depth methodology (dashed blue line).

to anomalous mass and it could be an error in source volume estimation because source strength is better constraint by displacements. Pressure and mass increment decreases as topography is taking into account while the depth of the source is increased in order to match the observed data. Thus choosing the right model to invert deformation and gravity data is a critical step in the interpretation of volcanic processes.

6. Conclusions

[25] We have shown that topography can significantly affect the surface gravity change predicted by intruded masses and pressurized magma reservoirs. Superposition of both sources illustrates the relative importance of topographic and self-gravitation effects. Topography reduces gravity magnitude as source depth increases with relief elevation and increases the thickness of the region where gravity changes vary. In this way, the magnitude and pattern of changes in gravity do not depend only on the source depth. Relief elevation also affects the characteristics and the change in the gravity signal, particularly when the lateral extension of the relief and the source depth are of the same order of magnitude.

[26] Self-gravitation cannot be safely ignored in computing gravity changes in half-space models when a gravitational source of mass is present. Nevertheless, self-gravitational effects are generally much smaller than the effects related to topographic relief for volcanic sources located at typical depths. Thus it is advantageous to use the reduce system formed by equations (8) and (2) to compute the topographic influence on displacements and gravity changes. The topographic effect can be approximated by summing (1) the free-air effect due to the uplift in a half-space deformation model with the source depth corrected for topography following *Williams and Wadge* [1998, 2000] and (2) the direct gravitational attraction of the

intruded mass, using the actual distance from source to the observation point.

[27] In this way, the interpretation of gravity changes would gain in accuracy through the use of a model that includes the topographic features of the medium, even though it is neglected in considering elastic-gravitational coupling. We have focused on the volcanic context because volcanic activity produces gravity changes that can be precursors of future eruptions and volcanoes are often associated with prominent relief. So, we have studied the gravity changes observed in Mayon volcano (Philippines) as an example. The inversion results have demonstrated that the depth, pressure and mass change can be altered to more closely match the observed data (the residual within data accuracy) when topography is taking into account.

Acknowledgments

[28] We wish to thank John Beavan, Louise Kellogg, and an anonymous reviewer for their thorough and constructive reviews and comments. The research of M.C. and J.F. was supported under MCyT projects REN2002-03450 and CGL2005-05500-C02/BTE. The research of F.L. was supported under MCyT project CGL2005-05500-C02/BTE and by the European Community with FEDER, the research team RNM-194 of Junta de Andalucía, Spain. The work of K.F.T. was performed under an NSERC Discovery Grant.

References

Battaglia, M., and P. Segall (2004), The interpretation of gravity changes and crustal deformation in active volcanic areas, *Pure Appl. Geophys.*, *23*, 231–247.

Bonaccorso, A. (1996), Dynamic inversion of ground deformation data for modeling volcanic sources (Etna 1991–93), *Geophys. Res. Lett.*, *23*, 451–454.

Bonafede, M. (1990), Axi-symmetric deformation of thermo-poro-elastic halfspace: Inflation of a magma chamber, *Geophys. J. Int.*, *103*, 289–299.

Cayol, V., and F. H. Cornet (1998), Effects of topography on the interpretation of the deformation field of prominent volcanoes: Application to Etna, *Geophys. Res. Lett.*, *25*(11), 1979–1982.

Charco, M., J. Fernández, M. J. Sevilla, and J. B. Rundle (2002), Modelling magmatic intrusion's effects on the geoid and vertical deflection. Application to Lanzarote, Canary Islands and Long Valley Caldera, California, *Fis. Tierra*, *14*, 11–31.

Charco, M., J. Fernández, F. Luzón, and J. B. Rundle (2006), On the relative importance of self-gravitation and elasticity in modeling volcanic ground deformation and gravity changes, *J. Geophys. Res.*, *111*, B03404, doi:10.1029/2005JB003754.

Davis, P. M. (1986), Surface deformation due to inflation of an arbitrary oriented triaxial ellipsoidal cavity in an elastic half-space, with reference to Kilauea volcano, Hawaii, *J. Geophys. Res.*, *91*, 7429–7438.

Delaney, P. T., and D. F. McTigue (1994), Volume of magma accumulation or withdrawal estimated from surface uplift or subsidence, with application to the 1960 collapse of Kilauea volcano, *Bull. Volcanol.*, *56*, 417–424.

De Natale, G., and F. Pingue (1996), Ground deformation modeling in volcanic areas, in *Monitoring and Mitigation of Volcanic Hazards*, pp. 365–388, Springer, New York.

Fernández, J., and J. B. Rundle (1994a), Gravity changes and deformation due to a magmatic intrusion in a two-layered crustal model, *J. Geophys. Res.*, *99*, 2737–2746.

Fernández, J., and J. B. Rundle (1994b), FORTRAN program to compute displacement, potential and gravity changes due to a magma intrusion in a multilayered Earth model, *Comput. Geosci.*, *20*, 461–510.

Fernández, J., J. Rundle, R. Granell, and T. Yu (1997), Programs to compute deformation due to magma intrusion in elastic-gravitational layered earth models, *Comput. Geosci.*, *23*, 231–247.

Fernández, J., K. F. Tiampo, G. Jentzsch, M. Charco, and J. B. Rundle (2001), Inflation or deflation? New results for Mayon volcano applying elastic-gravitational modeling, *Geophys. Res. Lett.*, *28*, 2349–2352.

Folch, A., J. Fernández, J. B. Rundle, and J. Martí (2000), Ground deformation in a viscoelastic medium composed of a layer overlying a halfspace, *Geophys. J. Int.*, *140*, 37–50.

Haskell, N. (1953), The dispersion of surface waves on multi-layered media, *Bull. Seismol. Soc. Am.*, *43*, 17–34.

Jahr, T., G. Jentzsch, R. S. Punongbayan, U. Schreiber, G. Seeber, C. Völksen, and A. Weise (1998), Mayon Volcano, Philippines: Improvement of hazard assessment by microgravity and GPS measurements?, in *Proceedings of the International Symposium on Current Crustal Movement and Hazard Assessment*, vol. 61, pp. 599–608, Seismol. Press, Beijing.

Jentzsch, G., R. S. Punongbayan, U. Schreiber, G. Seeber, C. Völksen, and A. Weise (2001), Mayon Volcano, Philippines: Changes of monitoring strategy after microgravity and GPS measurements, *J. Volcanol. Geotherm. Res.*, *109*, 219–234.

Jentzsch, G., A. Weise, C. Rey, and C. Gerstenecker (2004), Gravity changes and internal processes: Some results obtained from observations at three volcanoes, *Pure Appl. Geophys.*, *161*, 1415–1431.

Love, A. E. H. (1911), *Some Problems of Geodynamics*, *Oxford Appl. Math. and Comput. Sci. Ser.*, Cambridge Univ. Press, New York.

McTigue, D. F. (1987), Elastic stress and deformation near a finite spherical magma body: Resolution of the point source paradox, *J. Geophys. Res.*, *92*, 12,931–12,940.

McTigue, D. F., and P. Segall (1988), Displacements and tilts from dip-slip faults and magma chamber beneath irregular surface topograhy, *Geophys. Res. Lett.*, *15*, 601–604.

Michalewicz, Z. (1992), *Genetic Algoritms + Data Structures = Evolution Programs*, Springer, New York.

Mogi, K. (1958), Relations of eruptions of various volcanoes and deformation of the ground surface around them, *Bull. Earthquake Res.*, *36*, 99–134.

Punongbayan, R. S., O. D. Pena, E. G. Ramos, J. V. Umbal, H. B. Ruelo, L. P. Bautista, and J. C. Tayag (1990), *Operation Mayon*, Philipp. Inst. of Volcanol. and Seismol., Quezon City, Philippines.

Rundle, J. B. (1980), Static elastic-gravitational deformation of a layered half space by point couple sources, *J. Geophys. Res.*, *85*, 5355–5363.

Rundle, J. B. (1981), Numerical evaluation of static elastic-gravitational deformation in a layered half space by point coupled sources, *Internal Rep. SAND81-2058*, Sandia Natl. Lab., Albuquerque, N. M.

Rundle, J. B. (1982), Deformation, gravity, and potential changes due to volcanic loading of the crust, *J. Geophys. Res.*, *87*(B12), 10,729–10,744.

Rymer, H., and G. C. Brown (1989), Gravity changes as a precursor to volcanic eruptions at Poás volcano, Costa Rica, *Nature*, *342*, 902–905.

Thompson, W. T. (1950), Transmission of elastic waves through stratified medium, *J. Appl. Phys.*, *21*, 89–93.

Tiampo, K. F., J. B. Rundle, J. Fernández, and J. Langbein (2000), Spherical and ellipsoidal volcanic sources at Long Valley Caldera, California using a genetic algorithm inversion technique, *J. Volcanol. Geotherm. Res.*, *102*, 189–206.

Tiampo, K. F., J. Fernández, G. Jentzsch, M. Charco, and J. B. Rundle (2004a), New results at Mayon, Philippines, from joint inversion of gravity and deformation measurements, *Pure Appl. Geophys.*, *161*, 1433–1452.

Tiampo, K. F., J. Fernández, G. Jentzsch, M. Charco, and J. B. Rundle (2004b), Volcanic source inversion using genetic algorithm and elastic-gravitational layered earth model for magmatic intrusions, *Comput. Geosci.*, *30*, 985–1001.

Torge, W. (1989), *Gravimetry*, Gruyter, New York.

Völksen, C., and G. Seeber (1995), Establishment of a GPS-based control network at Mayon Volcano, *Cah. Cent. Eur. Geodyn. Seismol.*, *8*, 99–113.

Williams, C., and G. Wadge (1998), The effects of topography on magma chamber deformation models: Application to Mt. Etna and Radar Interferometry, *Geophys. Res. Lett.*, *25*, 1549–1552.

Williams, C., and G. Wadge (2000), An accurate and efficient method for including the effects of topography in three dimensional elastic models of ground deformation with applications to radar interferometry, *J. Geophys. Res.*, *105*(B4), 8103–8120.

Williams-Jones, G., H. Rymer, and D. A. Rothery (2003), Gravity changes and passive SO_2 degassing at the Masaya caldera complex, Nicaragua, *J. Geotherm. Res*, 2582, doi:10.1016/S0377-0273 (03)00033-7.

Withman, C. S. (2005), Volcanic disasters and incidents: A new database, *J. Volcanol. Geotherm. Res.*, *148*, 191–233.